



**HAL**  
open science

## Large river offsets and Plio-Quaternary dextral slip rate on the Red River fault (Yunnan, China)

A. Replumaz, R. Lacassin, P. Tapponnier, P H Leloup

### ► To cite this version:

A. Replumaz, R. Lacassin, P. Tapponnier, P H Leloup. Large river offsets and Plio-Quaternary dextral slip rate on the Red River fault (Yunnan, China). *Journal of Geophysical Research*, 2001, 106 (B1), pp.819-836. 10.1029/2000JB900135 . insu-01891130

**HAL Id: insu-01891130**

**<https://insu.hal.science/insu-01891130>**

Submitted on 9 Oct 2018

**HAL** is a multi-disciplinary open access archive for the deposit and dissemination of scientific research documents, whether they are published or not. The documents may come from teaching and research institutions in France or abroad, or from public or private research centers.

L'archive ouverte pluridisciplinaire **HAL**, est destinée au dépôt et à la diffusion de documents scientifiques de niveau recherche, publiés ou non, émanant des établissements d'enseignement et de recherche français ou étrangers, des laboratoires publics ou privés.

## Large river offsets and Plio-Quaternary dextral slip rate on the Red River fault (Yunnan, China)

A. Replumaz,<sup>1</sup> R. Lacassin, P. Tapponnier, and P. H. Leloup

Laboratoire de Tectonique, CNRS UMR 7578, Institut de Physique du Globe de Paris, Paris

**Abstract.** Using multispectral SPOT images and 1/100,000 topographic data, we present an improved map of the active Red River fault zone between Midu (Yunnan, China) and Hanoi (Vietnam). The fault zone is composed of parallel strands, one of which, the Yuanjiang fault was previously undetected. There also appears to be a component of extension all along the fault zone. Such extension increases toward the SE, from Yunnan to the south China sea coast, and the vector describing the motion of south China relative to Indochina points within the N45°-135°E quadrant. We attempt to assess the Plio-Quaternary dextral slip rate on the Red River fault (RRF) by restoring large river offsets and searching for the largest, plausible one. Across much of Yunnan, the fault is perpendicular to local catchments that drain into the Red River. From precise mapping of the river courses on SPOT satellite images and on 1/100,000 topographic maps, numerous multiple offsets along the fault can be detected and reconstructed. The lack of correlation between the apparent offsets and the lengths of the rivers upstream from the fault suggests either that the drainage system was in large part established prior to the onset of dextral slip along the fault or that frequent captures have occurred. We thus try to find the best fit between series of river channels upstream and downstream from the fault by progressively restoring the dextral displacement in increments of 500 m, up to an offset of 50 km. For each increment we measure the misfits (root mean squares, RMS) between the upstream and downstream channels. The best fit and smallest RMS are obtained for an offset of  $25 \pm 0.5$  km that we interpret to represent the clearest, large right-lateral displacement recorded in the geomorphology along the active Red River fault. Since dextral motion is likely to have started around 5 Myr, the most probable average Plio-Quaternary slip rate on the fault is of order of 5 mm/yr. We attribute the apparent lack of seismic activity on a large stretch of the fault to millennial recurrence times between great earthquakes. Our study shows that relatively small drainage systems can keep a good record of fairly large cumulative fault offsets.

### 1. Introduction

The Red River fault (RRF), one of the largest strike-slip faults of Asia [e.g., Tapponnier and Molnar, 1977; Allen *et al.*, 1984], stretches more than 1000 km, from eastern Tibet to the Hanoi Basin in Vietnam, along the SW border of the South China or Yangzi Block (Figure 1). It is now clear that large-scale, left-lateral ductile shear has occurred along this fault zone concurrent with the Tertiary extrusion of Indochina [e.g., Tapponnier *et al.*, 1990; Leloup *et al.*, 1995]. By contrast, the present degree of activity of the RRF is poorly known and more debatable. The level of historical and instrumental seismicity has been significant on either side of the fault and along its northwestern strand, but no moderate and large earthquakes are reported SE of Midu along the main strands of the RRF (Figure 2) [Allen *et al.*, 1984; Guo *et al.*, 1986; Gu *et al.*, 1989]. Along this central part of the fault system, however, ongoing and Quaternary movement is attested to by sharp geomorphic fault traces, by numerous drainage offsets, and by well-preserved cumulative scarps [Allen *et al.*, 1984]. The right-lateral slip sense inferred from

the offsets is compatible with fault plane solutions of earthquakes that have occurred on parallel, adjacent faults [e.g., Tapponnier and Molnar, 1977; Allen *et al.*, 1984]. Such movement has been related to the contemporaneous, eastward extrusion of the South China block [Tapponnier *et al.*, 1982; 1986; Peltzer and Tapponnier, 1988; Peltzer and Saucier, 1996]. To assess the direction and amount of motion of that block, which are debated, one needs to determine the kinematics, slip rate, and total right-lateral offset on the RRF. However while  $\approx 700$  km of Oligo-Miocene sinistral offset are now fairly well documented [Leloup *et al.*, 1995], the total amount of right-lateral slip in the Plio-Quaternary is not known. Present-day slip rate estimates range between  $\approx 1$  mm/yr and  $\approx 1$  cm/yr [Allen *et al.*, 1984; Weldon *et al.*, 1994]. To better assess such pending issues, we present here new evidence concerning the geometry and kinematics of the active fault strands along the central and southern RRF zone. We place a lower bound on the finite amount of right-lateral slip by searching for the largest geomorphic offsets. Assuming such finite offsets to have accrued since reactivation of the RRF in a right-lateral sense, probably around 5 Ma [Leloup *et al.*, 1993; 1995], we derive an average Plio-Quaternary slip rate that places additional constraints on the contemporaneous kinematics and geodynamics importance of the fault.

Copyright 2001 by the American Geophysical Union.

Paper number 2000JB900135.  
0148-0227/01/2000JB900135\$09.00

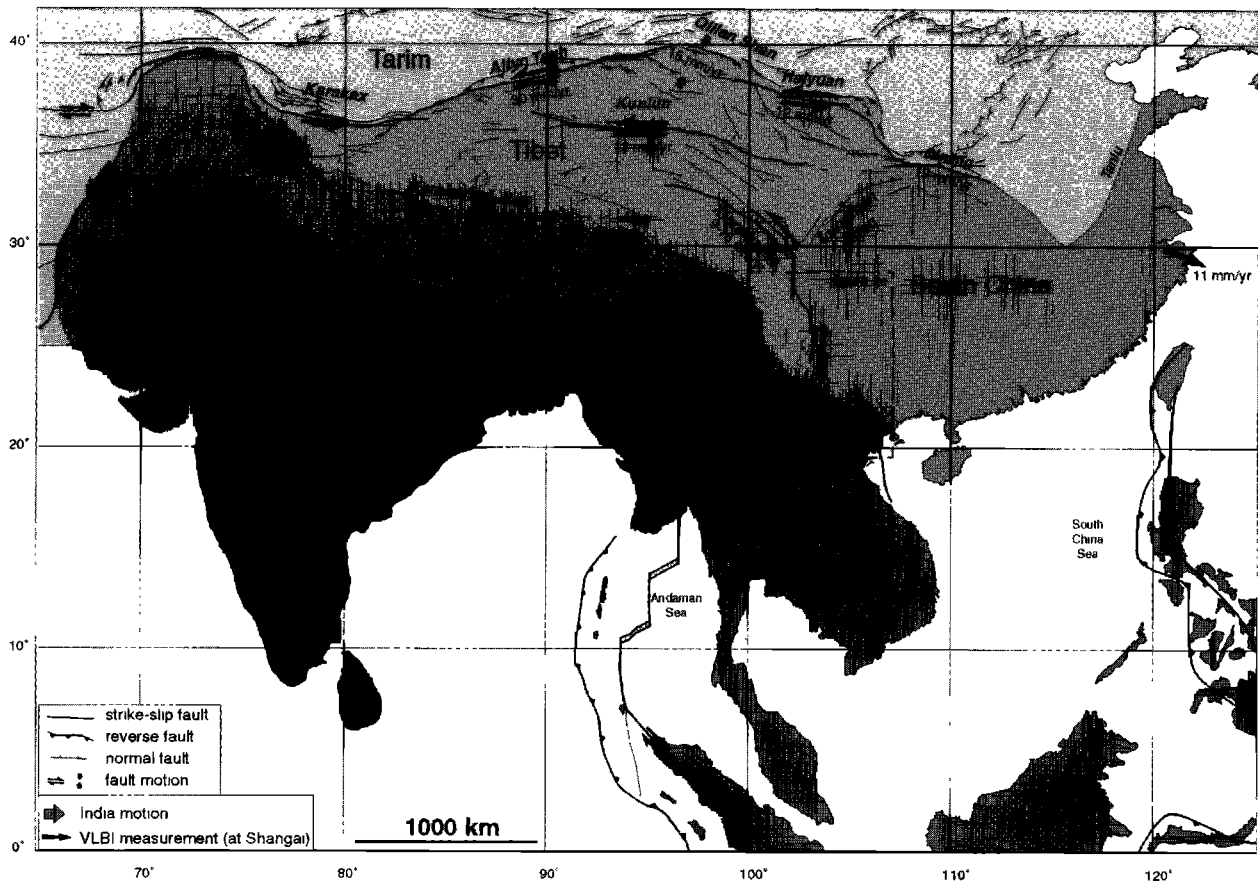


**Figure 1.** Schematic map of major active faults and continental blocks in eastern Asia. Fault slip rates and block motions are discussed in text. Red River fault slip rate is from this study.

## 2. Geodynamic Setting of the Red River Fault Zone

### 2.1. Oligocene Extrusion of Indochina Along the Ailao Shan-Red River Shear Zone

As India penetrated into Asia, from the Eocene ( $\approx 55$  Ma) onward, several continental blocks have been successively pushed toward the east, away from the frontal collision zone, along great strike-slip faults [e.g., *Tapponnier et al.*, 1986; *Peltzer and Tapponnier*, 1988; *Armijo et al.*, 1989]. Early on, the Red River fault zone, between south China and Indochina (Figure 1), guided Indochina's extrusion in the Oligo-Miocene [*Tapponnier et al.*, 1990; *Leloup et al.*, 1995]. Evidence for intense ductile shear is widespread in the narrow ( $< 20$  km wide) mylonitic gneiss cores of the Ailao Shan-Red River (ASRR) shear zone. Along this shear zone between  $\approx 35$  Ma and 15 Ma,  $700 \pm 200$  km of left-lateral movement occurred, concurrently with seafloor spreading in the South China Sea, at the southeastern tip of the zone [*Schärer et al.*, 1990; *Briais et al.*, 1993; *Leloup et al.*, 1993; *Schärer et al.*, 1994; *Leloup et al.*, 1995]. Normal components of motion on the RRF brought the mylonitic cores to the surface in two phases. The first phase of uplift, chiefly southeast of Midu, was due to transtension during sinistral shear, while the second one started at the onset of the present-day right-lateral regime [*Leloup et al.*, 1993; 1995; *Harrison et al.*, 1996]. The great length of the ASRR shear zone, its considerable finite,

sinistral offset, and its thermomechanical structure imply that it probably cuts through the whole lithosphere [*Leloup et al.*, 1995]. The reactivated right-lateral RRF is localized mostly along one edge of the former sinistral, lithospheric shear zone.

### 2.2. Plio-Quaternary Active Faulting and Present-Day Extrusion of South China

As India continued moving north, it induced a second phase of extrusion, pushing Tibet and south China toward the east [e.g., *Tapponnier et al.*, 1982; 1986; *Peltzer and Tapponnier*, 1988].

Central Tibet presently moves northeastward between the left-lateral Altyn Tagh fault and the right-lateral Karakorum-Jiali fault zone (KJFZ, Figure 1) [*Armijo et al.*, 1989; *Avouac and Tapponnier*, 1993; *Peltzer and Saucier*, 1996]. From geomorphic studies, slip rates of the order of 3 cm/yr are inferred on the Altyn Tagh fault [*Peltzer et al.*, 1989]. A comparable slip rate has been estimated along the Karakorum fault [*Liu et al.*, 1992; *Liu*, 1993] decreasing to between 1 and 2 cm/yr [*Armijo et al.*, 1989] along the eastern part of KJFZ (Gyaring Co, Beng Co, and Jiali en echelon faults). Such estimated slip rates have so far provided the principal input to plate-scale kinematic models that solve for the directions and amounts of motion of the different blocks north of India. Relative to fixed Siberia, for instance, the Tibetan Block may move toward the NE at  $\approx 40$  mm/yr

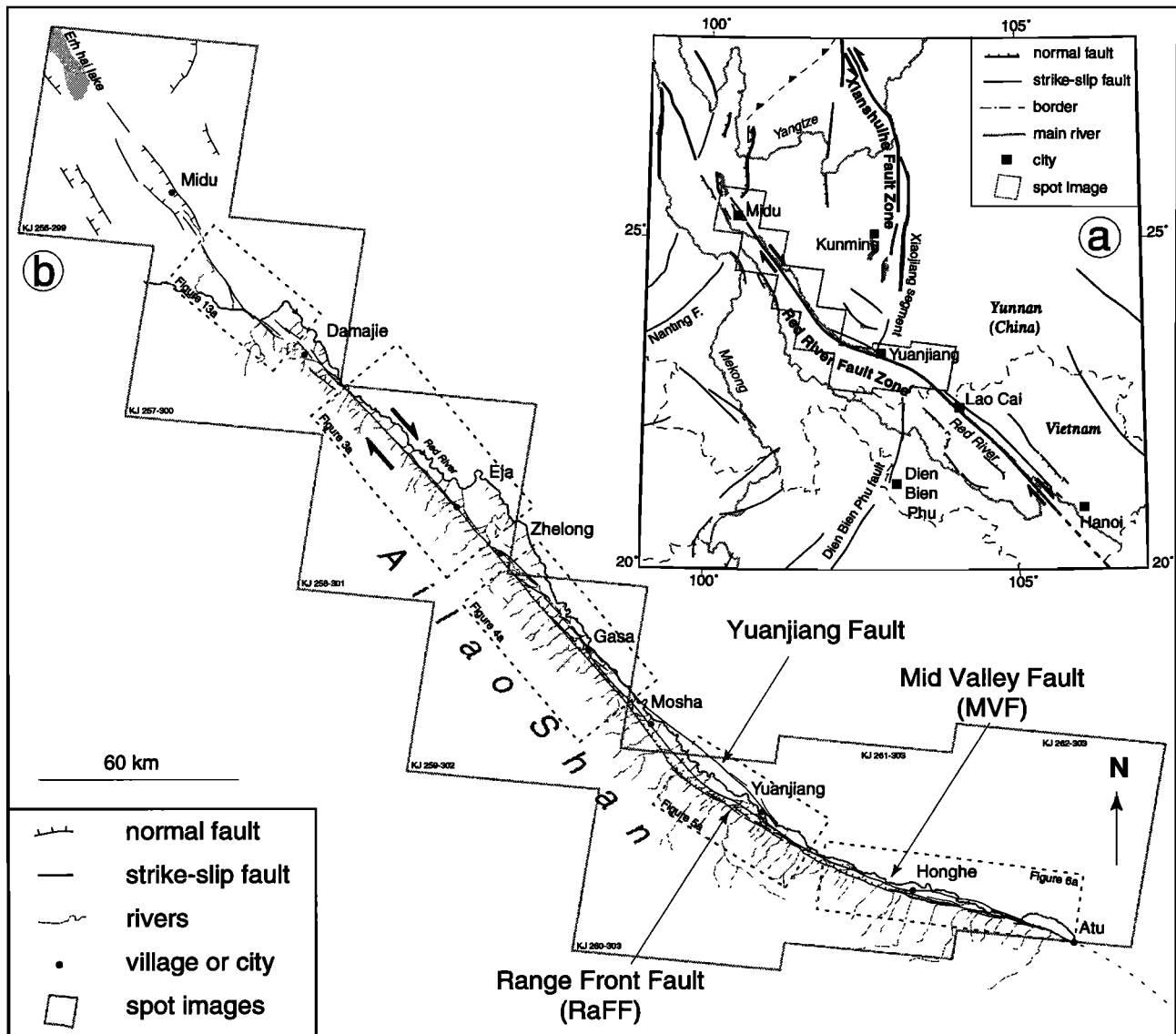


**Figure 2.** (a) Schematic map, from Landsat and SPOT images, of active faults in Yunnan Province (China) and Vietnam (redrawn from *Leloup et al.* [1995]). (b) Updated map of active fault traces along Red River fault zone, from SPOT images (KJ number reported on Figure).

[*Armijo et al.*, 1989; *Avouac and Tapponnier*, 1993] or at 30 to 35 mm/yr [*Peltzer and Saucier*, 1996]. Toward the east, such motion is transformed into clockwise rotation of the blocks separated by the Xianshuihe, Kunlun, and Haiyuan faults [*England and Molnar*, 1990] and into eastward motion of the eastern boundary of these blocks (Lungmen Shan, Figure 1) [*Avouac and Tapponnier*, 1993]. Thrusts along the Lungmen range seem to absorb little of this eastward motion ( $<5$  mm/yr, [*King et al.*, 1997]). East of this range, the South China Block thus moves east-southeastward, between the right-lateral RRF, southeastern continuation of KJFZ [*Tapponnier et al.*, 1986; *Armijo et al.*, 1989] and the left-lateral Qinling faults [*Peltzer et al.*, 1985], possibly at a rate of  $12 \pm 4$  mm/yr relative to north China [*Zhang et al.*, 1995]. The motion of south China relative to Siberia has been hotly debated. A rate of 1 to 1.5 cm/yr [e.g., *Avouac and Tapponnier*, 1993; *Peltzer and Saucier*, 1996] would imply

significant present-day extrusion outside of the collision zone. Very Long Baseline Interferometry (VLBI) measurements at Shanghai (Figure 1), near the northeastern edge of the South China Block, imply a rate of  $\approx 1.1$  cm/yr relative to Siberia [*Heki*, 1996] compatible with this interpretation. Others authors [e.g., *England and Molnar*, 1990; *Molnar and Gipson*, 1996], however, still contend that most of the eastward motion of Tibet is exaggerated, or absorbed along the eastern edge of the plateau. Clearly, direct knowledge of the slip rates along the RRF and Sagaing fault are needed to constrain this problem further.

Today, slip rate estimates on the RRF range loosely between 1 and 10 mm/yr. This wide range of values (1 order of magnitude) mainly arises from the difficulty of assessing the ages of offset geomorphic markers. In Yunnan, *Allen et al.* [1984] have documented numerous river offsets, ranging between 9 m and 6 km along the fault trace. With an offset of

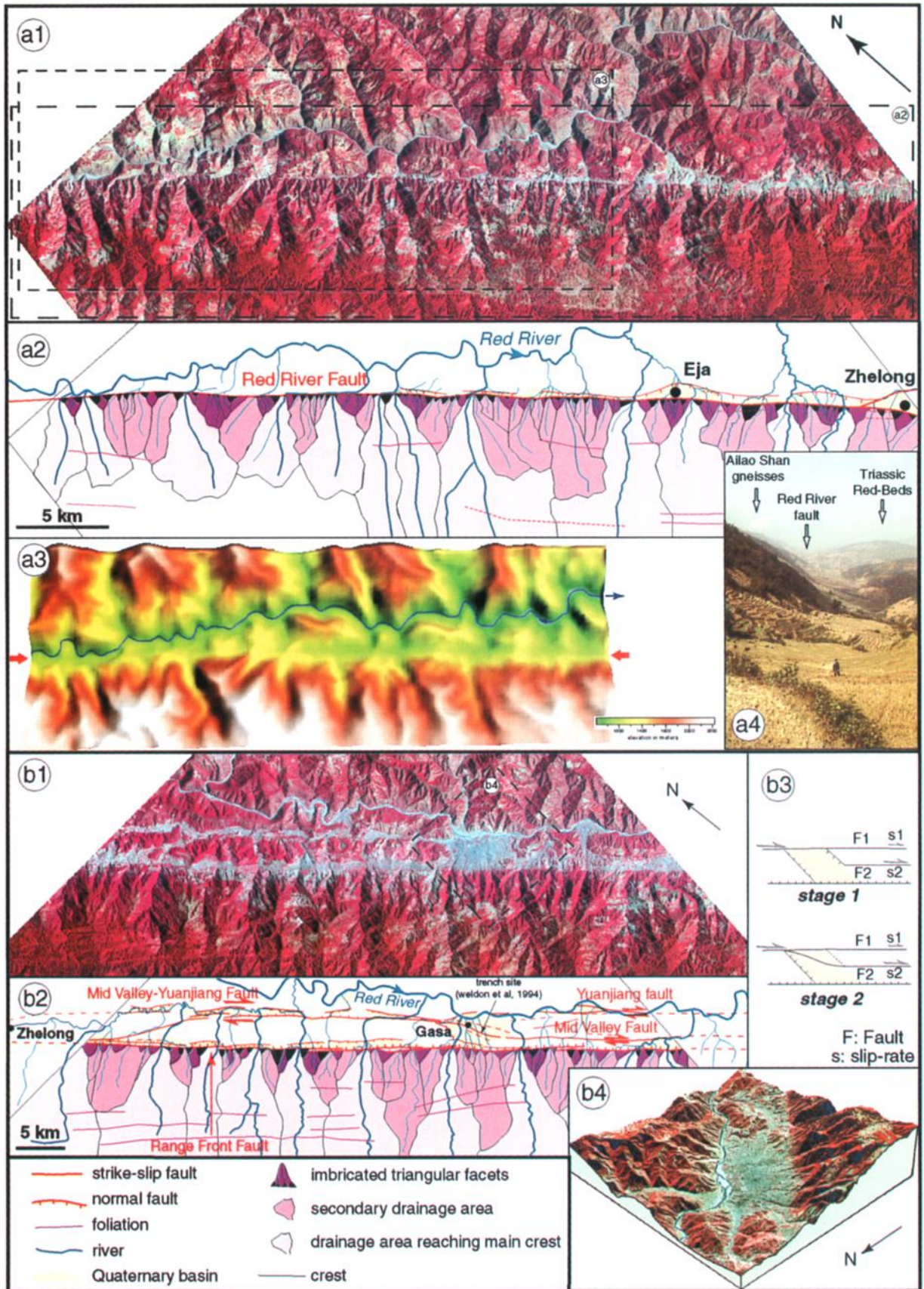


**Plate 1.** (a) Eja stretch of the RRF zone. (a1) SPOT image (KJ 258-301). (a2) Corresponding map. (a3) DEM. (a4) RRF trace looking northward of Eja. (b) Gasa stretch. (b1) SPOT image (KJ 259-302). (b2) Corresponding map. (b3) Sketch showing evolution of the "junction" basin due to interaction and slip transfer between strike-slip and normal fault stands. (b4) SPOT image of Gasa basin wrapped on DEM. (DEM from 1/100,000 topographic map).

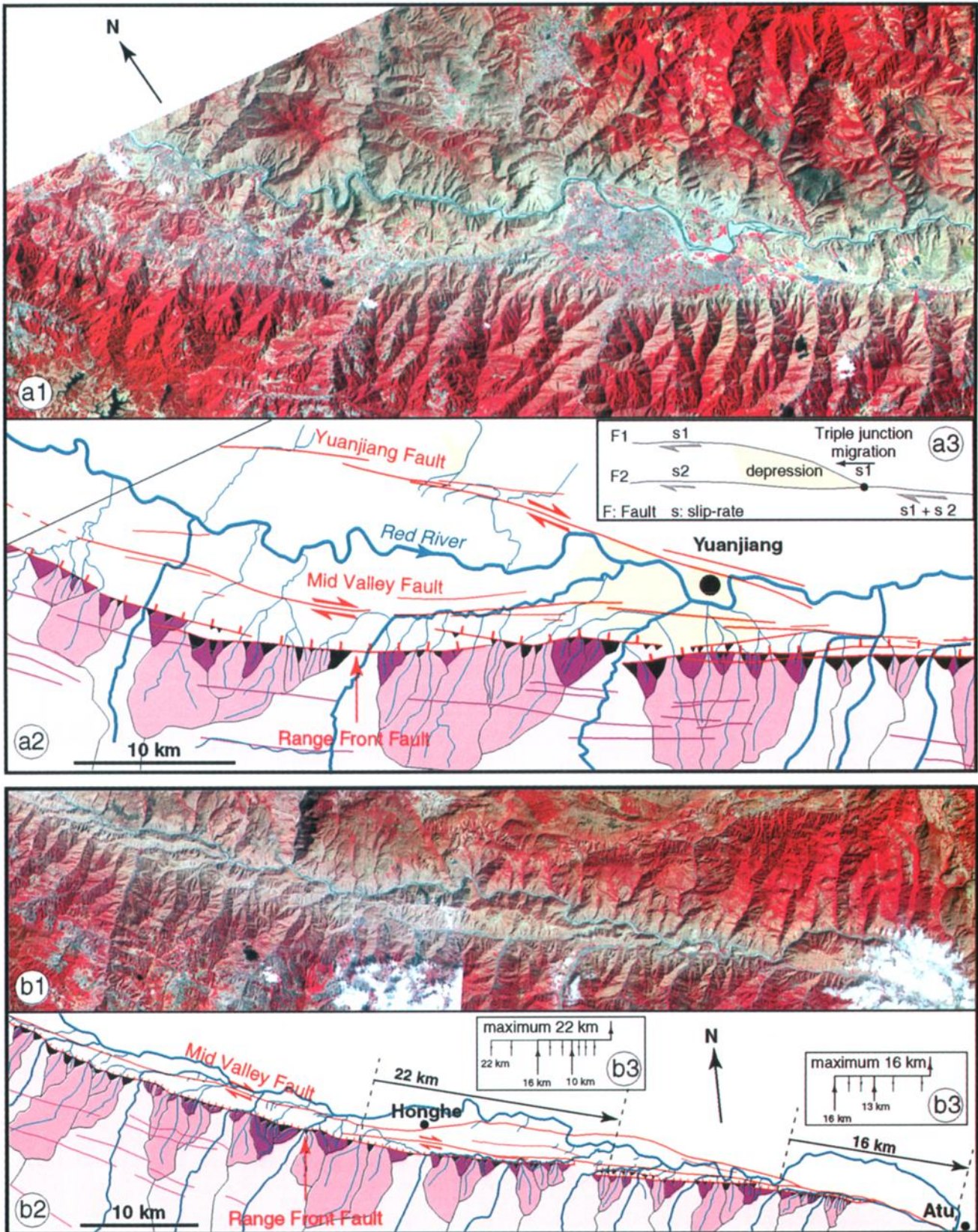


**Plate 2.** Same symbols as for Plate 1. (a) Yuanjiang stretch of the RRF. (a1) SPOT image (KJ 260-303). (a2) Corresponding map. (a3) Interpretation of the "junction" basin due to interaction and slip transfer between strike-slip fault stands at Yuanjiang. (b) Honghe-Atu stretch of the RRF. (b1) SPOT image mosaic (KJ 261-303 and 262-303). (b2) corresponding map. (b3) Largest offsets observed on Mid Valley fault, with their different significance.

5.5 km they were able to restore the deflected course of the Red River at one key site and the continuity of most of its tributaries. However values derived for the slip rate depend on inferences made on the age of the offset river channels. Using various assumptions for the rates and ages of rivers incision, *Allen et al.* [1984] inferred recent slip rates along the RRF to be at least 2 mm/yr and possibly  $\geq 7$  mm/yr. At one site near Gasa, *Weldon et al.* [1994] trenched a small stream channel offset by  $\approx 56$  m. Carbon 14 dating of alluvium within the channel ( $\approx 22$  kyr) implies a maximum slip rate of 2.7 mm/yr and, according to *Weldon et al.*, a probable rate of order of 1 mm/yr on the studied fault strand. On the SE part of the RRF in Vietnam the results of conventional and Global Positioning System (GPS) geodetic measurements are compatible with a strike-slip rate of between 1 and 5 mm/yr, with large uncertainties [*Duong and Feigl*, 1998]. Finally, the kinematic model of *Peltzer and Saucier* [1996] predicts  $10 \pm 5$  mm/yr of extensional motion oblique to the RRF trace with a dextral slip rate component of  $7.5 \pm 4$  mm/yr.

### 3. Geometry and Kinematics of the Active Red River Fault

#### 3.1. Overall Geometry of the Fault

On Landsat images and large-scale topographic maps the RRF displays continuous and linear traces between Midu and the Yunnan-Vietnam border (Figure 2) [*Tapponnier and Molnar*, 1977; *Allen et al.*, 1984; *Leloup et al.*, 1995]. From Zhelong to Atu the fault has two main parallel strands, the Mid Valley fault (MVF) and the Range Front fault (RaFF) [*Allen et al.*, 1984]. The RaFF follows the northeastern foot of the Ailao Shan range and separates the high-grade Ailao Shan gneisses from schistose sedimentary rocks (mostly Mesozoic red beds) to the north. The MVF cuts these sedimentary rocks a few kilometers north of the RaFF. Northwest of Midu, the fault trace becomes more complex [*Allen et al.*, 1984; *Leloup et al.*, 1995], with oblique, left-stepping normal faults and numerous pull-apart basins, such as that of Er Hai lake (Figure 2). Still farther north, several strike-slip faults and bookshelf faulting on N-S normal faults probably transfer some right-lateral slip to the Jiali fault zone of eastern Tibet [*Armijo et al.*, 1989; *Leloup et al.*, 1995]. Southeast of Lao Cai (Figure 2a), in Vietnam, the RRF splays into two main, distinct faults, the Song Hong and Song Chay faults that bound SW and NE sides, respectively, of the Day Nui Con Voi metamorphic core [*Lacassin et al.*, 1994; *Leloup et al.*, 1995]. The Song Hong fault, which continues along the Red River valley, shows multiple, discontinuous fault strands, while the Song Chay fault is simpler and more linear.

Between Midu and Atu, and in NW Vietnam, detailed mapping of the active fault traces on SPOT satellite images and topographic maps reveals that the active RRF zone, and particularly the MVF, is more complex than previously inferred. We thus first summarize below our new observations and their implications on the kinematics of the RRF, before analyzing in greater detail the magnitudes of right-lateral offsets of the drainage system.

#### 3.2. Red River Fault in Yunnan

Between Damajie and Zhelong (Figure 2b), for  $\approx 80$  km, the north central part of the RRF is made of a single strand, remarkably linear, that follows the base of the steep, 200 to 800 m high, triangular facets that bound the northeastern

flank of the Ailao Shan (Plate 1a). As elsewhere along the RaFF, such facets and the corresponding topographic relief, imply a dip-slip component of movement on the fault. The imbricated faceted spurs (purple on Plate 1, a2) are incised by small rills and separated by deeper canyons commonly with a wine glass geometry where they intersect the fault [*Allen et al.*, 1984]. The watersheds of these canyons often have a triangular shape and outline larger, less steep and more degraded facets (Plate 1, a1-a2). These larger facets are in turn separated by the first-order, deeply entrenched, tributaries of the Red River that flow down from the interior of the Ailao Shan, perpendicular to the fault. In contrast with the canyons that incise the faceted spurs, such first order rivers extend south of the steep northern flank of the Ailao Shan. Their catchments reach the main crest of the range (Plate 1, a1-a2). As they cross the fault, most of the largest rivers are offset right-laterally, with characteristic apparent offsets ranging typically between 1 and 3 km and up to 6 km (Plate 1, a1-a2). They form dogleg valleys along the fault trace for several kilometers, then swing back perpendicular to the fault to flow into the Red River. Smaller streams tend to flow into the fault-parallel dogleg valleys along the base of the facets. The dogleg valleys are separated by low passes floored with alluvial deposits (Plate 1, a4) and thus tend to form a continuous topographic trough along the fault trace (Plate 1, a3-a4). Toward the south, near Eja, this depression becomes a secondary, elongated basin with a small antithetic fault along its northeastern edge (Plate 1, a2). Toward the north, near Damajie, the fault splits into several strands, across an  $\approx 2$  km wide deformed zone (Figure 2). There rivers are clearly offset 3 to 6 km, but their dogleg shapes are smoother than farther SE, possibly because slip is partitioned between the several parallel strands. NW of Damajie the RRF, the northwest end of the trace (Figure 2b), crosses the Red River course, which is offset by  $\approx 5.5$  km [*Allen et al.*, 1984]. North of the intersection with the Red River and up to Midu, the RRF trace is rather linear and displays small river offsets of only several hundred meters to 1 km [*Allen et al.*, 1984].

From Zhelong to Atu (Figure 2b), the Range Front fault (RaFF) follows continuously the base of the Ailao Shan. In detail, the trace of this fault, which is sharp along most of its length and marked by triangular facets, is composed of stepping segments (Plates 1 and 2). As observed NW of Zhelong, the facets are made of imbricated faceted spurs and attest to dip-slip motion. From NW to SE, the heights of the facets decrease from  $\approx 1700$  m (Zhelong - Gasa), to 1300 m (Gasa - Yuanjiang), and finally to 900 m (Yuanjiang - Honghe), which suggests a southeastward decrease of the vertical cumulative offset as the fault veers to a more easterly direction. The fault trace is generally very linear across transverse topography, implying a rather steep fault plane. The existence of small V-shaped deflections, for instance, northwest of Honghe (Plate 2b), however, indicates that the fault dips to the north, consistent with a component of normal slip. In contrast with what is observed along the Damajie-Zhelong segment, most rivers do not show clear dextral offsets at the base of the relief where they cross the RaFF.

The Mid Valley fault (MVF) is located 1 to 3 km NW of the RaFF (Figure 2b). On SPOT images the trace of this fault does not appear to be as simple as previously inferred from Landsat images and air photographs [*Allen et al.*, 1984]. In many places, it forms a  $\approx 1$  km wide zone marked by several stepping or parallel strands (e.g. between Honghe and Atu,

Plate 2b). As discussed below, we infer the Yuanjiang and Gasa depressions to have formed where such fault strands interact and meet (Plate 1, b3; Plate 2, a3). Systematic horizontal offsets of river valleys and intervening crest lines are observed across the MVF. There is little topographic evidence, on the other hand, of significant cumulative vertical offset on this fault. Between Honghe and Atu, most of the large tributaries of the Red River show right-lateral offsets of between 3 and 10 km, often associated with large shutter ridges (Plate 2b). Two of the main tributaries that follow the RaFF east of Honghe and west of Atu show particularly large apparent offsets of 22 and 16 km, respectively (Plate 2b, b3). In this zone the offset Red River tributaries flow parallel to the southernmost strand of the MVF but not exactly on it. This fault strand offsets by  $\approx 100$  m the second-order streams that incise the shutter ridges located between the Red River and the fault.

Using multispectral SPOT images, we mapped, mostly on the left bank of the Red River, a previously unrecognized active fault strand, the Yuanjiang fault. It extends from Gasa to Yuanjiang, shortcutting the most curved bend of the RRF (Figure 2b). As along the MVF, river deflections indicate a dextral sense of movement on the Yuanjiang fault, but with smaller apparent offsets, up to  $\approx 3$  km only (Plate 2a). The two most important basins along the central stretch of the RRF, the Yuanjiang and Gasa basins, are located where the Yuanjiang fault meets the MVF. The Yuanjiang basin (Plate 2a) is bounded to the north by the Yuanjiang fault, which merges with the MVF a few kilometers SE of the basin. It is limited by the RaFF to the south. We interpret this flat, triangular depression to be a "junction" basin due to local extension, as part of the right-lateral slip on the MVF is transferred to the Yuanjiang fault (Plate 2, a3). The Gasa basin, which displays the more rhombic shape of a pull-apart basin (Plate 1, b4), is probably also an extensional sag due to dextral slip transfer between the RaFF and the MVF to the SW and between the MVF and Mid Valley-Yuanjiang fault to the NE (Plate 1, b3). Just west of Gasa, the Yuanjiang fault and MVF merge to form a more conspicuous 1-km-wide linear fault zone. This zone meets the RaFF  $\approx 35$  km NW of Gasa [Allen *et al.*, 1984], though one splay continues in the same direction as far as Zhelong.

### 3.3. Red River Fault in Vietnam

East of Atu, the principal RRF trace is linear and channels much of the present-day Red River course. West of Lao Cai, the RRF splays again into two main faults, the Song Hong and Song Chay faults, along the SW and NE of the Day Nui Con Voi gneiss range, respectively (Figure 3).

The Song Hong fault zone, which is in line with the main RRF trace east of Atu, is composed of closely spaced parallel strands (Figures 2 and 3). The Red River meanders in a 2 to 4-km-wide trough limited by these strands and filled by Neogene and Quaternary sediments. We interpret this trough to be a narrow, elongated graben reflecting components of normal throw on those strands, consistent with the fact that the RRF swings back to a more southerly direction east of Atu. That such normal throw is recent is attested to by the presence of uplifted terraces and flat abrasion surfaces, as well as by the 1460-m-high cumulative relief along the southwestern border of the Day Nui Con Voi range. Within

this uplifted horst of metamorphic rocks, narrow ridges outlining the steep foliation formed by Tertiary sinistral shear [Leloup *et al.*, 1995] are clear on SPOT images and in the field. The foliation is nearly parallel to the Song Hong fault, and in places, foliation surfaces stand out in the morphology and are marked by vertical scarps. This suggests recent reactivation of foliation planes by normal movement. North of the Day Nui Con Voi crest line, down to the NE, movement is clear on such planes, but there is little evidence of vertical motion on the Song Chay fault itself. This fault, marked by an outstanding strike-slip furrow along most of its length, has a linear trace with segments up to 100 km long. Along both the Song Hong and Song Chay faults, there are numerous right-lateral river offsets that range between  $\approx 300$  m and 2 km, even though they are less clear than in Yunnan [Lacassin *et al.*, 1994]. Toward the SE, both faults may be followed some distance into the Quaternary deposits and across the rice paddy fields of the Hanoi Basin. They become undetectable in the Red River delta.

North of the Song Chay fault, the Song Lo-Tam Dao fault shows a discontinuous trace composed of several stepping segments (Figure 3). Near Tuyen Quang, one such segment offsets right laterally the Song Lo river by  $\approx 3$  km. Southeast of Tuyen Quang, the presence of spectacular triangular facets and the  $\approx 1500$ -m-high relief of the Tam Dao range require a component of normal motion on the Tam Dao fault, consistent with its more southerly strike.

South of the Song Hong fault, normal throw is also clear on the Phan Si Pang-Phu Luong faults, which form the SW limit of the Hoang Lien Son mountains (Figure 3). The Phan Si Pang granite range, of Tertiary age, reaches 3143 m and displays spectacular pinnacles, needles, and deeply incised canyons. This indicates fairly rapid uplift and recent erosion. The southwestern flank of this range is bounded by a cumulative scarp that shows steep,  $\approx 700$  to 1000-m-high, imbricated faceted spurs. Flat basins filled with Quaternary deposits lie along the base of this scarp. To the southeast, discontinuous right-lateral en echelon segments connect the Phan Si Pang fault with the Phu Luong fault. The trace of the latter fault, which to the south also limits a  $\approx 1000$ -m-high relief bounded by triangular facets, is less clear on satellite images than that of the Phan Si Pang fault.

North and east of the Song Hong-Song Chay faults, there is evidence for active folding, related to right-lateral motion on NW-SE trending strike-slip faults (Figure 3). For instance, the NW-SE striking Cao Bang fault, which is roughly parallel to the RRF, has a sharp linear trace in the morphology, with little evidence of dip-slip motion. East of Lang Son, a growing E-W trending anticline (1540 m, Figure 3) that folds Mesozoic beds branches eastward from this fault, consistent with ongoing dextral slip on it. To the south, other east to NE trending, apparently growing folds, possibly in connection with dextral strike-slip motion, follow the coast of the Gulf of Tonkin (Bac Bo) north of Halong Bay. The fold trends, outlined on satellite images by bedding, curve clockwise southwestward when approaching the RRF (Figure 3). Finally, Recent SW-NE trending folds are clear on seismic profiles in the northern gulf of Tonkin (Figure 4) [Replumaz, 1994]. Like those onshore, these folds, which lie just northeast of the continuation at the sea of the Tam Dao and Song Chay faults, probably absorb part of the contemporaneous dextral motion on them.

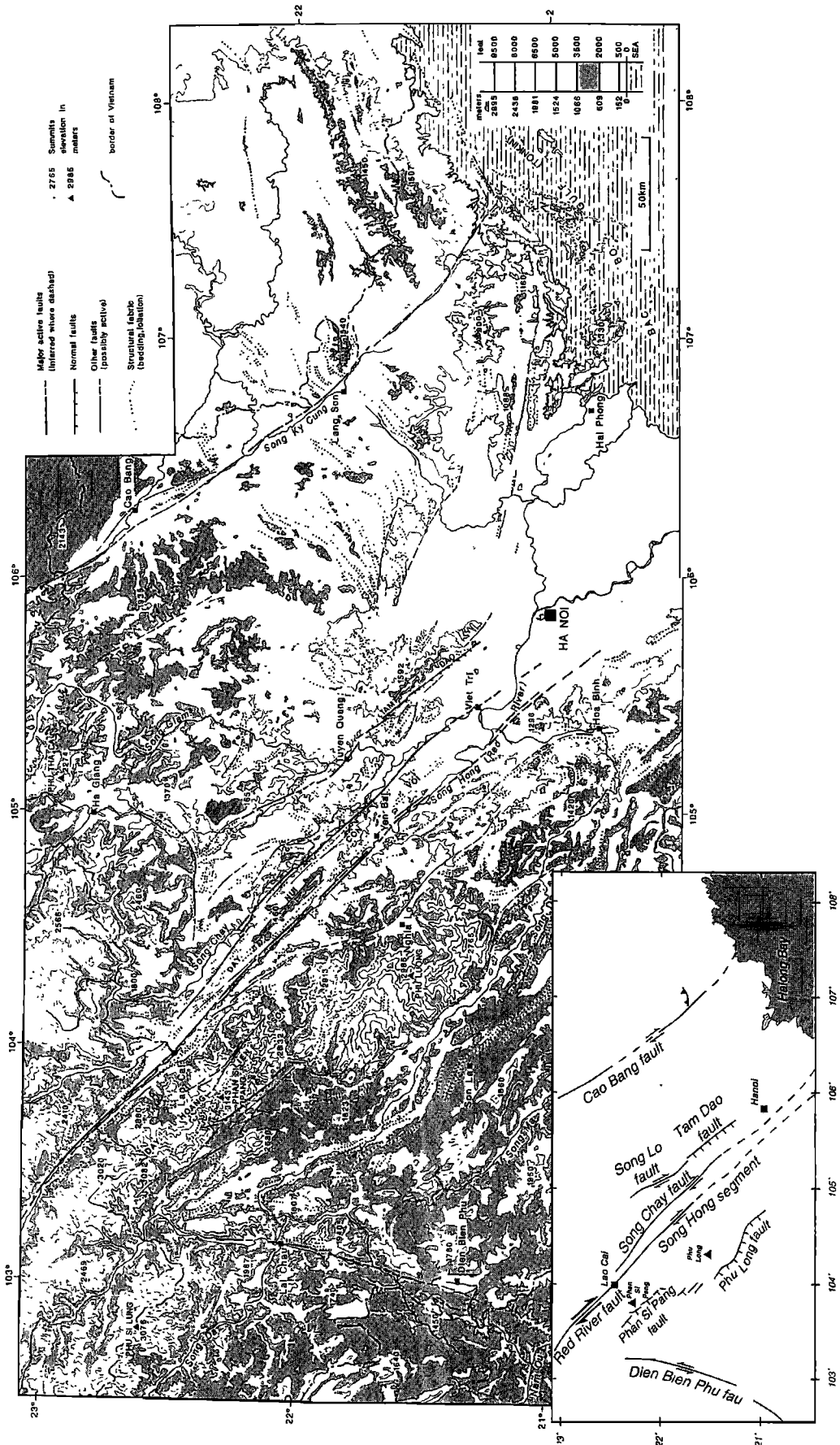
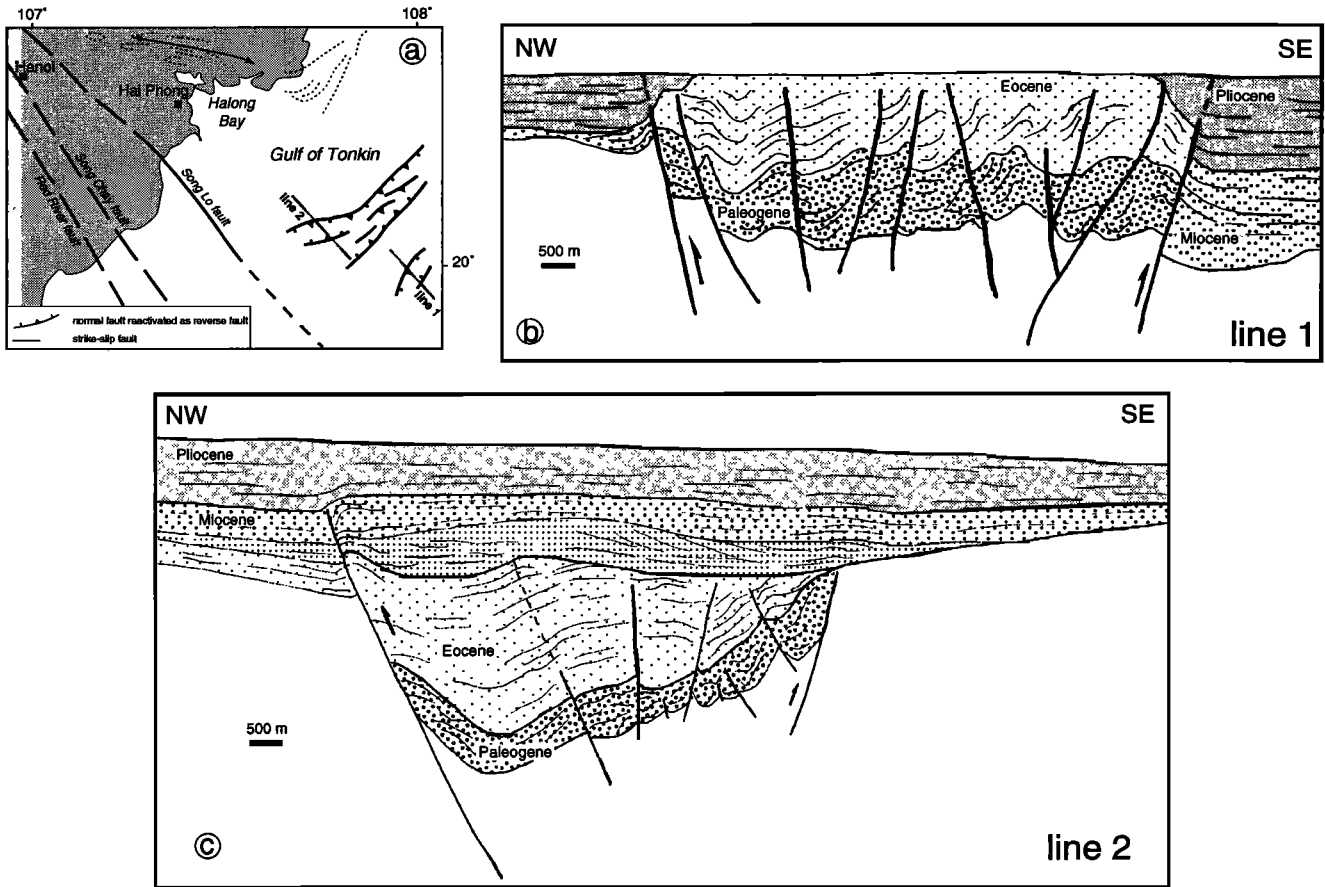


Figure 3. Seismotectonic map of northern Vietnam. Topography is from Tactical Pilotage Chart (TPC) 1/500 000 maps. Fault traces and structural fabrics are drawn from interpretation of Landsat and SPOT images.



**Figure 4.** Location (a) and interpretation of two seismic lines (line 1 (b), line 2 (c)) in the Gulf of Tonkin, showing tectonic inversion of graben. Inversion occurred sometime after Pliocene unconformity.

**4. Correlation Between River Size and Offset**

Mapping of fault traces along the RRF shows that over most of its length, it is not a simple fault system, as long recognized by *Allen et al.* [1984]. In particular, the strike-slip component is commonly partitioned between several fault strands (e.g., MVF, Yuanjiang, RaFF strands; Song Hong and Song Chay strands). Only between Damajie and Zhelong, along the base of the Ailao Shan, is there a single fault trace (Figure 2). Along this 80 km stretch of fault, the trace cuts the valleys of deeply entrenched tributaries of the Red River, which flows a few kilometers north of the fault. This section of the fault is thus the best place to search for maximum right-lateral offsets recorded in the morphology. Though somewhat more complex, the stretch between HongHe and Atu shows prominent single river deflections that reach 16 to 22 km. After testing the reality of such large offset values, we search for the most likely maximum offset that may be deduced from the river network.

Because they continuously adapt their course to tectonic movement, rivers are lateral slip markers that must be used with caution. Typically, rivers may form large meanders, smooth fault-induced deflections, or be captured by adjacent streams. In many cases, however, large rivers seem to be offset by a greater amount than small ones, so that there appears to be a correlation between river length upstream from a strike-slip fault and river offset [e.g., *Gaudemer et al.*,

1989]. This may be interpreted to reflect the fact that large river courses are older and generally more stable than smaller ones. This is also consistent with the fact that rivers lengthen their watersheds progressively by headward retreat while the

**drainage area (km<sup>2</sup>)**

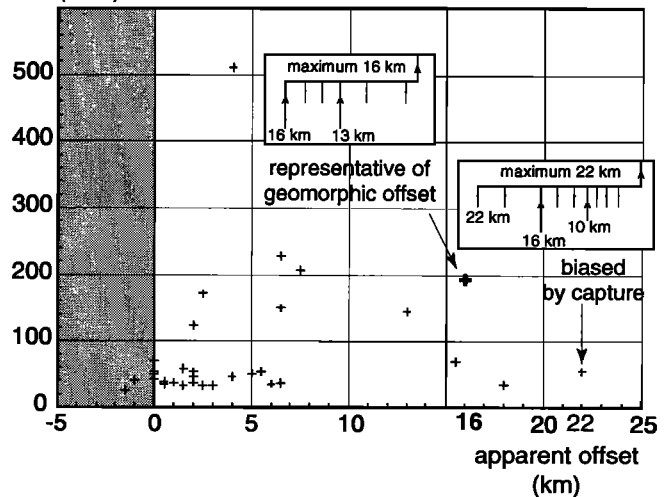


**Figure 5.** Plot of the drainage areas >15 km<sup>2</sup> as a function of apparent river offsets. Offsets are mostly right lateral (80% of 32 rivers). See text for discussion.

fault keeps moving. That large rivers are less susceptible to capture than smaller ones may also partly account for the river size versus offset correlation. To search for such a correlation along the RRF, we plotted the offsets as a function of upstream catchment area (Figure 5).

There is a big difference in the size of the Red River tributaries in the Damajie-Zhelong (northern) region and the Zhelong-Atu (southern) region. In the northern region the rivers have small drainage catchment areas ( $<100 \text{ km}^2$ ) and small apparent offsets ( $<10 \text{ km}$ ). In the southern region the rivers have the largest drainage areas (up to  $500 \text{ km}^2$ ) and are offset up to  $22 \text{ km}$ . The disparity of the relief is probably the main reason for this difference. In the north the river beds are steep and deeply incised, but the growth of the drainage is limited by the narrow and high relief of the Ailao Shan. In the south the Ailao Shan is wider, its elevation is lower, and river catchments south of the RRF become larger. Plotting catchment areas as a function of apparent offsets shows a rough positive trend but no clear linear correlation (Figure 5). Large offsets ( $\approx 20 \text{ km}$ ) exist for rivers with relatively small catchment areas ( $<100 \text{ km}^2$ ). Such rivers may have been captured by larger ones that already had an offset. In that case, the apparent offset could be the sum of the offsets of the small river before capture and of the larger river. The maximum apparent offset measured near HongHe ( $\approx 22 \text{ km}$ ) might thus be larger than that due to fault slip (Plate 2, b3). The other large apparent offset ( $16 \text{ km}$ ), by contrast, is associated with a river with a larger catchment ( $\approx 200 \text{ km}^2$ ). This offset might be more representative of the actual geomorphic offset of rivers of this size in that region (Plate 2, b3).

In any event, the absence of a clear correlation between river size and offset implies that such a correlation might have been canceled by random processes, particularly river captures, during coeval fault and drainage evolution [Gaudemer *et al.*, 1989]. To understand the offsets of the Red River tributaries, we must therefore consider a model that takes into account the frequent occurrence of capture.

## 5. Strike-Slip-Driven Capture of Offset Drainage Systems

Let us consider a simple drainage system emplaced prior to, and offset passively by fault motion. The evolution and changes in river shape due to such motion may be illustrated by sliding past each other the upstream and downstream sides of the corresponding three-dimensional (3D) elevation model of topography and drainage (Figure 6). The river drainage network chosen consists of three rivers of the same size that are deeply entrenched in the topography and thus are unable to shift their courses on their own. Capture occurs only when the downstream channel of one river becomes aligned with the upstream channel of another. For amounts of slip smaller than river spacing, the rivers are simply deviated along the fault, forming sharp dogleg kinks across its trace, whose lengths are equal to cumulative fault slip (Figure 6a). The identical river offsets are thus actual offsets, all of them in the dextral sense of motion. As cumulative slip increases (Figure 6b), one upstream channel (B) can be captured by a downstream channel of comparable or greater size and hence entrenchment depth (C'). The new river course thus formed (B+C') will show negligible or even negative, i.e., apparently

sinistral, offset (Figure 6b). Further increments of slip across this new channel will restore a dextral offset, albeit smaller by the spacing between B and C', than the actual offset by the fault (e.g., B' and C', Figure 6c). The downstream channel abandoned during the first capture event (B') may eventually be reused when it comes in line with an upstream channel with comparable or smaller entrenchment depth (e.g. A, Figure 6c). Therefore, as fault slip becomes larger than the average channel spacing, few rivers will follow their initial downstream channels. Captures thus make finite offsets difficult to measure when they are greater than the maximum river spacing [Peltzer *et al.*, 1988], and river dogleg kinks tend to define variable apparent offsets smaller than the actual finite offset of the drainage network. However, the hierarchy and irregular spacing of streams of various sizes and entrenchments, which can be preserved on either side of the fault, may be used to restore the network's initial geometry. In nature, as in the simple example of Figure 6, the spacing pattern of the upstream channels (A, B, C) should generally remain correlated to that of the downstream channels (A', B', C') especially if the channels are entrenched. Matching downstream and upstream sets of irregularly spaced rivers of variable sizes and entrenchments should thus help to estimate the maximum offset recorded by the drainage network, which should be greater than river spacing and all other apparent offsets.

Note that on the model of Figure 6, the interplay of river offset and capture results in the formation of a narrow furrow following the fault. This furrow locally corresponds to abandoned, perched, dogleg segments of former valleys. Such a furrow is particularly clear in the field and on the digital elevation model (calculated from digitized 1/100 000 Chinese topographic maps) of the region between Damajie and Zhelong (Plate 1, a3-a4). The small rounded hills between the fault furrow and the Red River, probably correspond to segmented shutter ridges. Both the presence of this furrow and the lack of correlation between river size and offset are telltale signs of the importance of capture and of finite offsets of the drainage system greater than the apparent river offsets in that region (maximum  $8 \text{ km}$  between Damajie and Zhelong).

## 6. Search for Large River Offsets Along the Red River Fault in Yunnan

In the example of Figure 6, it remains possible, despite the occurrence of two captures, to restore the initial geometry of the drainage by sliding back the two sides displaced by the fault. Can one similarly retrieve the most plausible, initial geometry of the Red River tributaries by correlating river channels across the RRF?

### 6.1. Geomorphic Evidence for a 25-km Dextral Offset Along the Red River Fault

Using the topographic map of the Damajie-Zhelong region (Figure 7a) and sliding back the Ailao Shan footwall of the RRF, SW of the fault trace, we tried to find acceptable fits between the downstream and upstream channels of the Red River tributaries (Figure 7b). Since the apparent offsets are variable, canceling some of them does not provide a satisfactory restoration of the entire drainage. The best qualitative fit of the drainage network however is obtained by

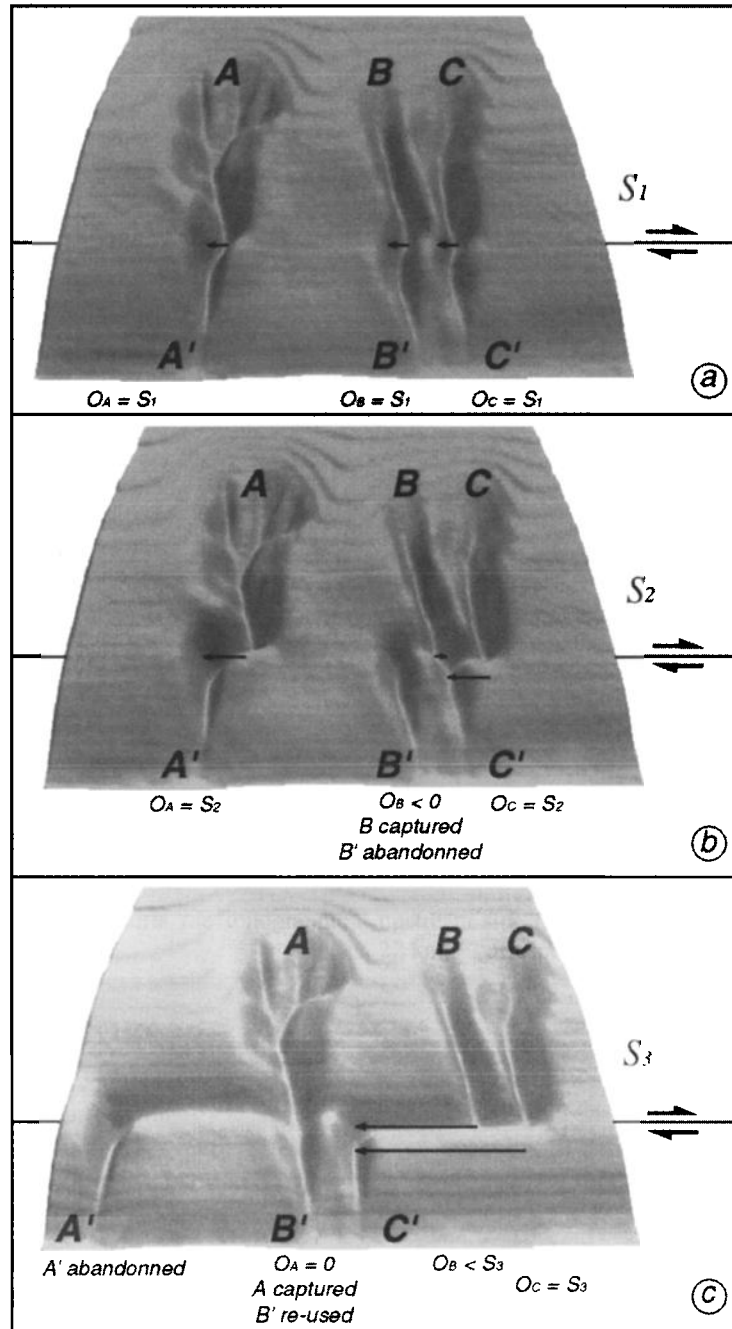


**Figure 6.** Sketches of 3-D drainage system perturbation by strike-slip fault with increasing fault displacement from (a) to (c). DEM is derived from a simplified topographic map. Successive stages are obtained by cutting and sliding initial map, restoring by hand continuity of topographic contours, and interpolating new contours to produce the next DEM. ( $O_X$ , offset of river channel X;  $S_i$ , slip along fault at stage  $i$ ). See discussion in text.

sliding the Ailao Shan side of the fault 25 km southeastward. Restoring this amount of cumulative dextral slip on the RRF leaves little residual offset along a segment more than 50 km long, shown on Figure 7b. No large abandoned downstream channel or dammed upstream channel remains. All the reconstructed river courses are fairly straight, and the network geometry looks essentially unperturbed. Cutting and sliding back the corresponding SPOT image mosaic by 25 km also yields a good qualitative fit and supports the topographic evidence (Figure 7, c and d).

## 6.2. Systematic Test of Offsets Between 0 and 50 km

To strengthen further our interpretation, we try to assess whether the restoration discussed above is statistically acceptable and unique. We systematically tested all possible offsets between 0 and 50 km by increments of 0.5 km. For each increment, we calculated the misfit between upstream and downstream channel sets. We used segments of the upstream side of the fault of increasing length: successively 22 km, corresponding to five river channels, 50 km,

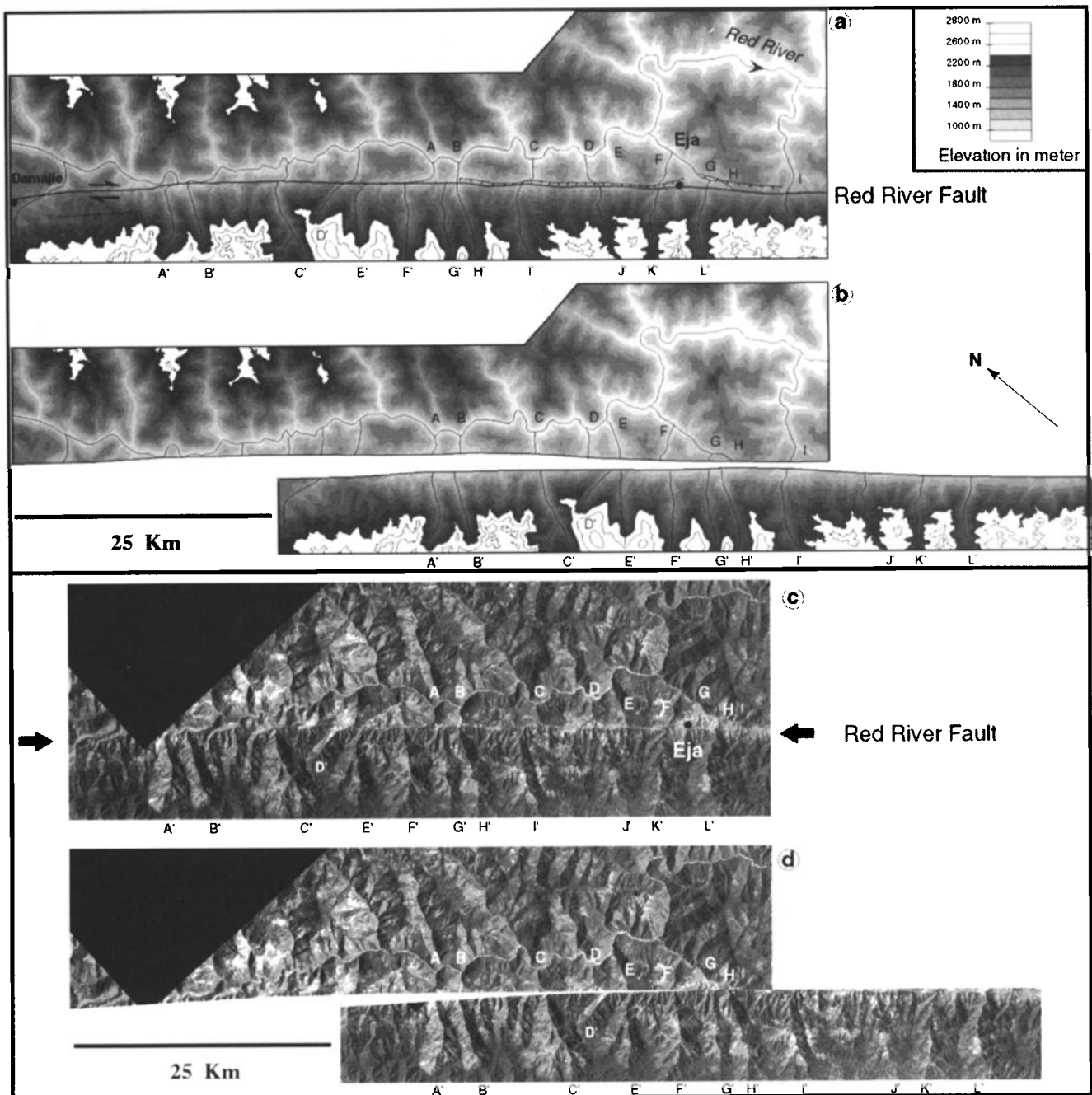


**Figure 7.** (a) Topographic map (from 1/100,000 Chinese maps) of RRF Eja stretch (portion of reconstructed zone). First-order Red River tributaries are indicated by letters. (b) Topographic map cut along RRF and slid back 25 km. (c) mosaic of SPOT images (KJ 257-300 and 258-301) of approximately same area. Second-order tributaries, incising facets, are also visible. (d) SPOT image cut and slid back 25 km.

corresponding to 10 channels, 85 km, corresponding to 15 channels. The associated downstream segment needed is  $85 + 50 = 135$  km long. The first 60 km of the fault used are shown on Figure 7 (with the upstream rivers A' to L' (upstream rivers 1' to 12'), and downstream rivers A to I (downstream rivers 1 to 9)).

The abscissa of each channel is measured along the fault from an arbitrary origin. The motion on the fault is modeled by moving the upstream block to the right which is equivalent to add slip increments to upstream channels abscissa. We thus

restore progressive dextral displacement on the fault. For each of the 100 iterations the distance  $\Delta$  between one upstream channel and the closest downstream channel is measured. This distance is the smallest geometrically possible offset, positive or negative, for one upstream channel. For each iteration we calculated the root mean square (RMS) of the  $\Delta$  values obtained for each channel. Then we plot the RMS obtained for each iteration.

For calibration, we first apply this calculation to an unperturbed drainage network that we correlate with itself.

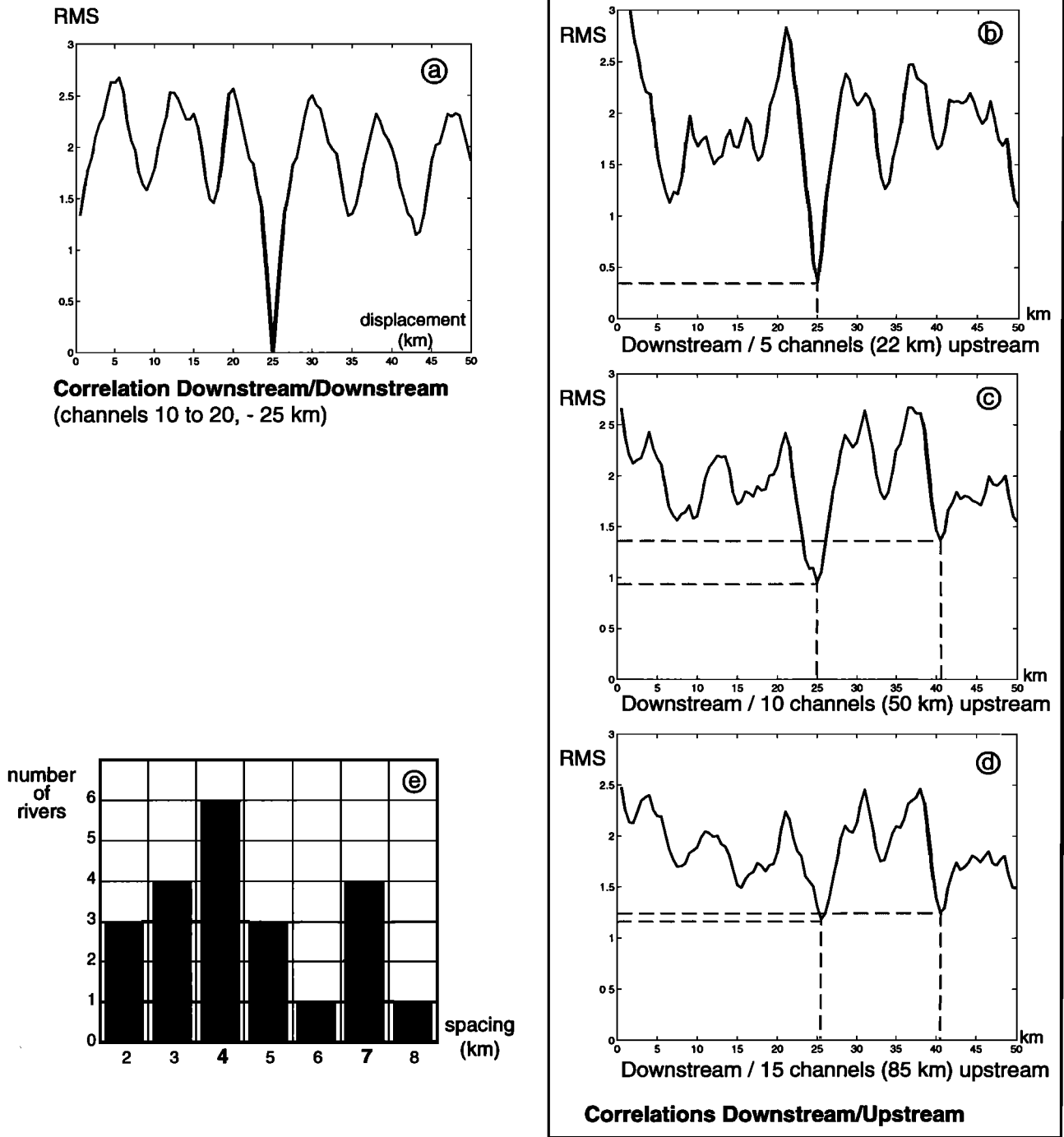


**Figure 8.** (a) Calibration test on artificial perturbation of drainage network obtained by offsetting, then correlating the downstream side with itself. (b) to (d) Correlation between downstream side and upstream side. Restored displacements along RRF versus root mean square (RMS) of distances between each upstream channel and closest downstream channel. (e) Histogram of spacing of upstream rivers showing main peak at 4 km and smaller one at 7 km.

We used as an unperturbed network a section on the downstream side of the fault. We correlate the entire downstream section (rivers 1 (or A) to 50) with the central downstream part (rivers 10 (or J) to 20), which have been moved by 25 km to the left, which is equivalent to introducing an artificial fault displacement. The result of this simulation is shown on Figure 8a. The RMS values oscillate between 1.5 and 2.5, with a mean value around 2. The RMS

graph shows a clear periodicity, about 8.5 km (peaks at 8.5, 17, 25, 34, 42.5 km), probably corresponding to the periodicity of the drainage. The RMS equals zero only for an offset of 25 km, corresponding to that artificially introduced in the simulation.

Thus calculating the RMS parameter evolution for a drainage perturbed by a fault should permit assessment of the total displacement of the drainage, which gives a stronger

signal than the periodicity of the drainage. A RMS parameter equal to zero represents a perfect fit, restoring an unperturbed drainage system with straight river courses crossing the fault without deviation. In nature, this is an improbable circumstance and a good fit between the upstream and downstream sides will simply be marked by a minimum of the RMS parameter. A maximum of the RMS, by contrast, signals a bad fit that leaves important residual offsets of the river courses.

We have done three correlations of the downstream side with the upstream side of the fault for 5, 10, and 15 upstream channels (Figures 8b, 8c and 8d). The rivers 1' to 5' (A' to E', Figure 7) are along an homogeneous section where the corresponding downstream side (A to E) is not very wide and where the downstream channels (A to E) are straight and perpendicular to the fault trace. For rivers 6' to 10' (F' to J', Figure 7) the corresponding downstream side (F to J) of the relief becomes wider, and the downstream channels F to J are not perpendicular to the fault anymore. For rivers 11' to 15' (southeast of Eja), the corresponding downstream side is wider, and the downstream and upstream sides are separated by a basin elongated along the fault (Plate 1, a1-a2). The correlation done with 5 and 10 channels appears to confirm the existence of a 25-km offset, marked by clear RMS minimum peaks. On this fault section (rivers A' to J', Figure 7) the position of the channels thus appears to record an offset larger than any apparent offset of individual river courses (Figure 6). Between 0 and 50 km, there is no better fit than that qualitatively detected by sliding back the topographic maps and SPOT images (Figure 7). For this offset the residual misfit is very low (minimum RMS values lower than 0.5 for five channels (Figure 8b) and lower than 1 for 10 channels (Figure 8c). The correlations done with 10 and 15 upstream channels (Figures 8c and 8d) also show a second minimum peak, corresponding to an offset of 41 km, with a RMS value lower than 1.5, less than the RMS value related to drainage periodicity in the simulation case (Figure 8a).

The statistical tests of Figure 8 thus support the tectonic interpretation derived from matching the topography and SPOT image (Figure 7). They also imply that this interpretation is unique and that the uncertainty on the fault offset is small  $\pm 0.5$  km. The significance of the second peak is less clear. As it appears on a different section of the fault (southeast of channel E'), it could signal a larger offset, recorded by a different, more ancient part of the drainage network.

On the three graphs of Figures 8b, 8c and 8d the secondary minima are fairly regularly spaced with a pseudo-period of  $\approx 8$  km. This value is similar to the periodicity found in the simulation of Figure 8a, though the distribution of the peaks is less regular (Figure 8a). This pseudo-periodicity is not well correlated with preferred values of the spacing of upstream drainage channels. The histogram of the upstream river spacing shows a broad peak centered at 4 km and a smaller, narrower one at 7 km (Figure 8e).

### 6.3. Is a 25-km Offset Valid Everywhere in Yunnan ?

It is difficult to make as quantitative a test as that performed on the Damajie-Zhelong stretch elsewhere along the RRF. On other stretches of the fault the strike-slip component becomes partitioned between the Range Front fault (RaFF), and the Mid Valley Fault (MVF) or Yuanjiang

fault. Across the MVF, the rivers, which are less entrenched into smoother relief, are more susceptible to change their courses than between Damajie and Zhelong. Moreover, as the Red River is often very close to the MVF, downstream channels can be very short and difficult to map. Nevertheless, the largest apparent offset of 16 km, and even the more speculative one of 22 km, between Atu and Honghe (Plate 2, b3), are close to the 25 km offset determined near Eja.

North of Damajie, the Red River itself crosses the RRF trace and may have been offset by  $\approx 20$  km [Leloup *et al.*, 1995]. We infer that the broad and deeply incised Shuitian valley, presently occupied by a small south flowing river, is a former, abandoned course of the Red River (Figure 9a). From elevation contours on the 1/100,000 topographic maps, the present reversed slope gradient along the Shuitian river amounts to  $<200$  m, except close to the Red River, which could be due to recent regressive erosion. Removing an offset of 20 km would restore a straight Red River course (Figure 9c). Capture of the Red River's upstream catchment by one of its downstream tributaries may thus have occurred (Figures 9d and 9e). Only after this capture would the Red River course have accrued the 5.5 km right-lateral offset reported by Allen *et al.* [1984]. Note that the 41 km offset also corresponds with a plausible  $43 \pm 3$  km offset of the Red River valley [Leloup *et al.*, 1995].

## 7. Summary and Discussion

### 7.1. RRF Geometry and Kinematics

From central Yunnan to the Red River delta and Vietnamese coast, detailed mapping of the RRF zone shows that it includes several active strands [Allen *et al.*, 1984; Leloup *et al.*, 1995; this study]. Along much of the fault, the relief and morphology of the Ailao Shan and Day Nui Con Voi range fronts imply that a component of extension occurs perpendicular to the fault, particularly where it strikes NW-SE. In Yunnan, along the Damajie-Zhelong segment, and along the Range Front fault south of Zhelong, prominent triangular facets attest to the corresponding normal component of motion (Plates 1 and 2). Farther south, in Vietnam, there is also evidence of active normal faulting on the RRF or parallel to it. Elongated Neogene basins extend along the fault zone and normal faulting occurs on prominent faults parallel to the RRF (e.g., Phan Si Pang and Tam Dao faults). At the SE tip of the RRF, the Red River delta (Hanoi Basin) lies within a strongly subsident basin with buried grabens filled by a thick Neogene sequence. This implies that the component of extension increases towards the SE, from NW Yunnan to the South China Sea coast [e.g., Tapponnier *et al.*, 1986; Leloup *et al.*, 1995].

The present dextral strike-slip component of motion is clearly demonstrated by the existence of numerous river offsets [Tapponnier and Molnar, 1977; Allen *et al.*, 1984; this study]. North of Zhelong, all the river offsets are located along the base of the faceted Ailao Shan range front (Plate 1, a1-a2). South of Zhelong, dextral slip is distributed on several strike-slip fault strands up to a few kilometers north of the Range Front fault (Plates 1b and 2). This geometry is the same as that found, over a shorter length, along the Nyainqentangla range front and Damxung half graben in Tibet [Armijo *et al.*, 1986]. As proposed by Armijo *et al.* [1986], two distinct fault strands at the surface may be due to

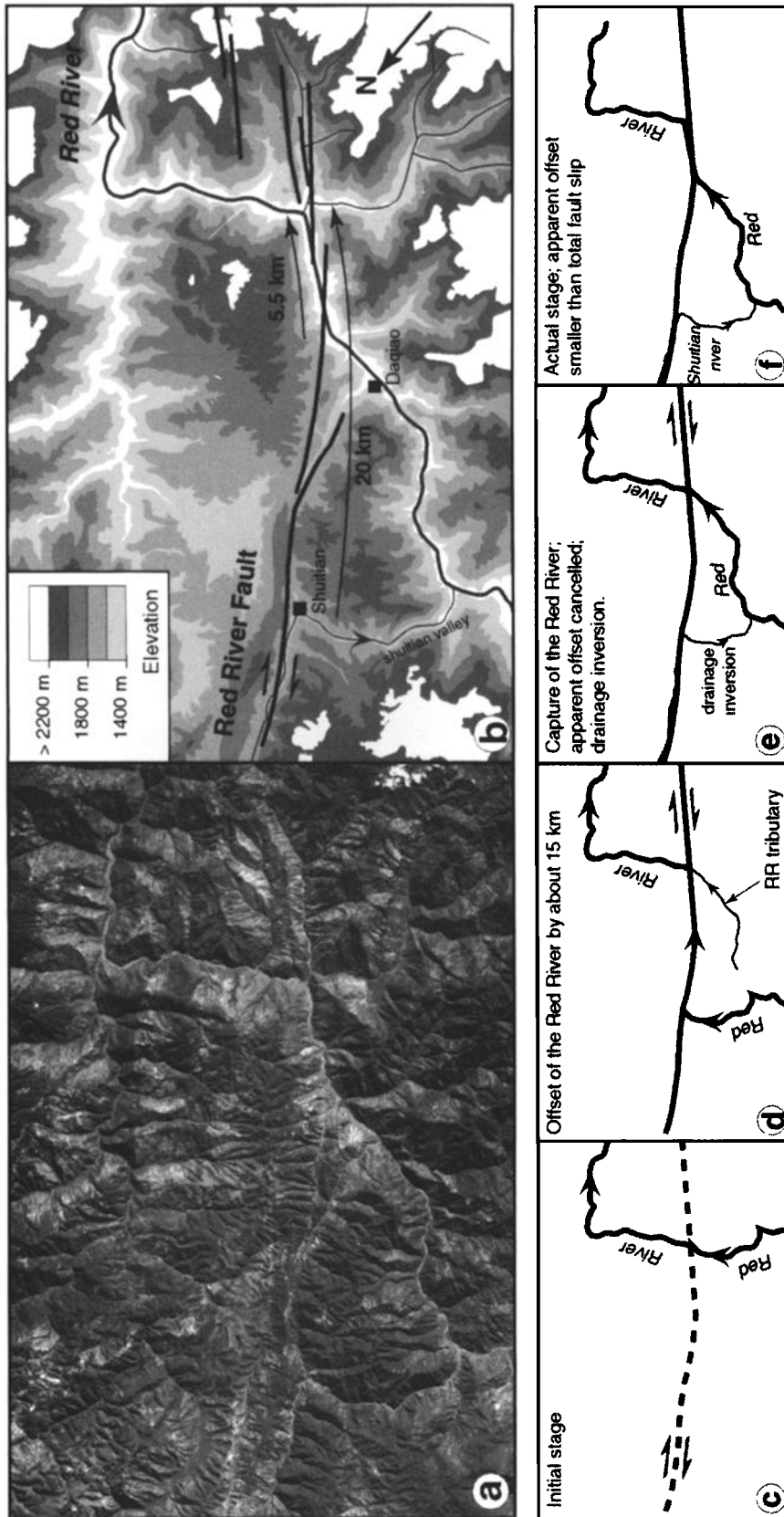
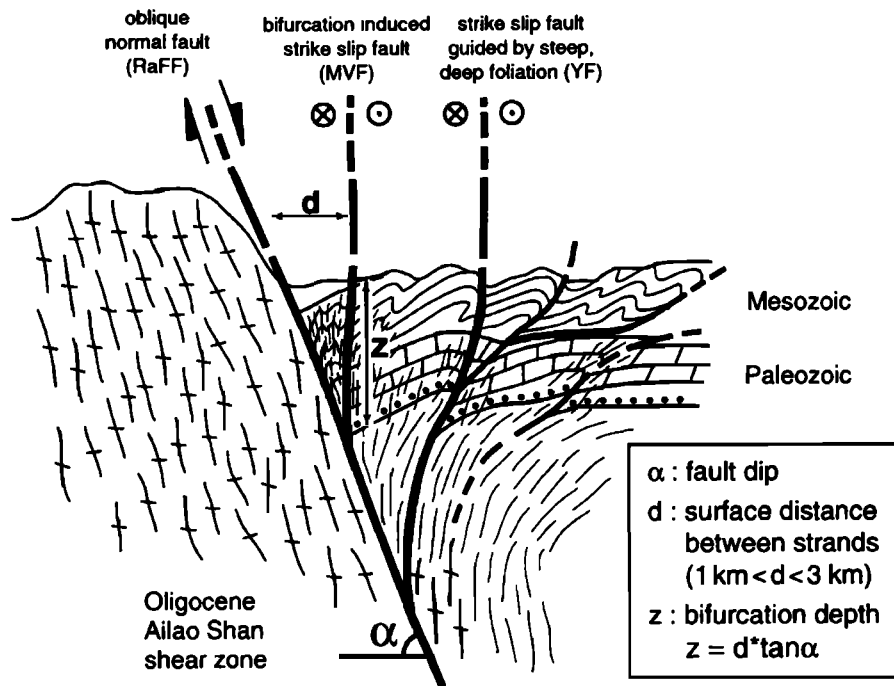


Figure 9. (a) Detail of SPOT image (KJ 257-300) showing Red River fault bend and Shuitan valley. (b) Topographic map (from 1/100 000 chinese maps) and active fault traces; arrows show possible Red River offsets discussed in text. (c) to (f): Possible evolutionary sketches of Red River course during right-lateral motion.



**Figure 10.** Schematic cross-section showing separation into normal and strike-slip strands for fault with oblique motion at depth [after *Armijo et al.*, 1986]. Bifurcation point can be at one sedimentary interface in cover (Mesozoic red sandstones or calcareous Paleozoic).

bifurcation from a single reactivated fault plane with oblique motion at depth [Leloup, 1991]. Such motion is not transmitted rigidly into the weaker superficial layers (e.g., sediment), but partitions into oblique normal and pure strike-slip displacement along the bifurcation line (Figure 10). If this takes place along the RRF, then the fact that the horizontal distance between the normal and strike-slip strands varies between 1 and 3 km implies that there are important variations either in the dip of the fault plane or in the depth of the bifurcation line. Taking a nearly constant fault dip, between  $70^\circ$  and  $75^\circ$ , equal to that of the metamorphic foliation along the Ailao Shan range front, would imply that the depth of the bifurcation point varies between 3 and 11 km (Figure 10). Fault bifurcation at several levels within the shallow upper crust, corresponding to mechanical discontinuities such as decollements on key horizons within the sedimentary cover (unconformities of Devonian reds beds and limestones, of Mesozoic red sandstones, and of poorly indurated Neogene conglomerates) might account for the variable spacing between the RRF and MVF where that spacing is small. However, it seems doubtful that such a bifurcation mechanism operates at depths  $>10$  km. It is thus possible that some of the strike-slip strands of the fault system that lie farthest from the Range Front fault, particularly the newly discovered Yuanjiang fault, are guided by steep foliation in buried, hanging wall gneisses belonging to the Oligocene Ailao Shan shear zone [Leloup *et al.*, 1995]. *Gaudemer et al.* [1995] have suggested that along-strike strain heterogeneities in mid crustal, transcurrent shear zones might account for partitioning of slip between several active surface strands along the Haiyuan fault in Gansu province.

In any event, bulk motion along the RRF zone in map view appears to be generally oblique to the trend of the fault with

an angle that depends on that trend. This implies that the vector describing the motion of south China relative to Indochina points in a direction between  $N135^\circ$  (fault strike) and  $N45^\circ$  (normal to fault strike).

One particularly striking, large-scale feature of the RRF is the bend (Figure 2b) of the fault trace between Moshu and Atu [Allen *et al.*, 1984; Leloup *et al.*, 1995]. For  $\approx 120$  km the fault zone departs from its  $N130^\circ/140^\circ E$  overall trend to a more easterly strike  $N110^\circ/120^\circ E$ . Along this stretch of the fault zone, several strike-slip strands are observed, with one of them, the Yuanjiang fault, smoothing, and in part shortcutting, the sharpest, northern bend. This fault strand probably absorbs a significant part of the dextral motion, thus alleviating kinematic complexities due to the curvature of the bend. On a larger scale the Moshu-Atu region lies mostly east of the place where the left-lateral Xianshuihe (XSH) fault zone meets the RRF (Figure 2a). The Xianshuihe fault zone is one of the most seismically active strike-slip fault of China [Allen *et al.*, 1991]. In Tibet it shows clear evidence of Holocene motion [Allen *et al.*, 1991]. At its southern tip, in Yunnan, the fault splits into several strands (Anninghe, Zemuhe, and Xiaojiang faults) one of which (Xiaojiang fault) come to abut the RRF without crossing it (Figure 2a). Though the Dien Bien Phu fault, south of the RRF, has a trend and slip sense similar to that of the Xianshuihe fault, it lies east of the RRF-XSH intersection. Present-day motion along the Xianshuihe fault thus must be absorbed in the Yuanjiang region, as suggested by folding of Neogene conglomerates between Yuanjiang and Atu. It seems likely that such motion has distorted the RRF trace, creating its large-scale bend [Allen *et al.*, 1984]. This would resemble the Transverse Ranges bend of the San Andreas fault in relation to the Garlock fault.

## 7.2. Dextral Slip Rate on the RRF

In Yunnan, from geomorphic disturbances of the drainage network we document fairly robust evidence for a right-lateral offset of  $25 \pm 0.5$  km on the RRF. To deduce a slip rate from this value, constraints on the timing of the onset of dextral motion and on the age of the offset drainage are needed. Thermochronological dating of uplifted metamorphic rocks [Leloup *et al.*, 1994; 1995; Harrison *et al.*, 1996] and seafloor spreading kinematics in the South China Sea [Briais *et al.*, 1993] imply that left-lateral shear along the Ailao Shan shear zone ceased around 15 Ma. On the basis of the fast cooling episode found in the Diancang Shan [Leloup *et al.*, 1993] and Ailao Shan [Chen and Li, 1998], right-lateral motion on the RRF might have started around 5 Ma. There is additional evidence to support a  $\approx 5$  Ma onset of RRF dextral reactivation. North of Dali, extensional basins that formed at the northern tip of the RRF are filled with Pliocene (5.5 Ma) sediments [Academy of Geological Sciences of China, 1975]. To the southeast, in the Gulf of Tonkin, seismic lines (Figure 4) show normal faults perpendicular to the trend of the RRF with clear, systematic inversion starting around 5 Ma [Replumaz, 1994].

Whether the drainage network formed while the fault was moving dextrally or was already in place when it started to move affects any assessment of a rate from the offset value. That there is little difference between the reconstructed drainage pattern and an undisturbed one and that the same reconstruction applies to rivers that have different catchment areas suggest that the network was well established and had evolved before reactivation of the RRF in a dextral sense. In this event the age of dextral slip onset is the essential constraint to derive a slip rate from offset value. Taking the 25-km offset and a 5 Ma age for dextral reactivation would yield a slip rate of 5 mm/yr. Although this offset value is determined within  $\pm 2\%$ , the uncertainty on the age is poorly known. Thus the uncertainty on the slip rate can not yet be ascertained quantitatively.

An alternative hypothesis, which we consider less likely, is that the drainage formed and evolved rapidly to a differentiated, mature stage after reactivation of the RRF in a dextral sense. In this event, rapid incision and evolution of the drainage network would most likely be related to a strong, global change in climate, such as, for instance, the onset of the Quaternary glacial cycles around 2 Ma. With a drainage network entrenched in the topography around 2 Ma the slip rate deduced from the 25-km offset would be 12.5 mm/yr. Without direct radiometric dating of drainage incision we cannot discard this possibility, but we consider our first hypothesis to be more likely.

The rate we find most plausible (5 mm/yr) is within the bounds discussed by Allen *et al.* [1984] (between 2 and 7 mm/yr). It is greater than the maximum slip rate inferred from trenching at Gasa (2.7 mm/yr) [Weldon *et al.*, 1994]. This is probably because trenching there was performed on only one of the three different strands of the fault, in the middle of a pull-apart sag (Plate 1, b2).

A slip rate of 5 mm/yr implies that seismic hazard may be more important than hitherto thought on the Red River fault. No large earthquake, however, is known to have occurred on the fault between Midu and Hanoi in the instrumental and historical seismic record time spans. There are several possible explanations for this apparent quiescence. The RRF

might be creeping, but there is evidence for large fault scarps that attest to the occurrence of past earthquakes [Allen *et al.*, 1984]. The historical catalog of Chinese earthquakes, which spans nearly 3000 years (since 1180 B.C.), might be drastically incomplete since about 1500 A.D. in a sparsely populated mountain region, with no large city between Dali and Hanoi. Finally, and probably most likely, the RRF, like other strike-slip faults (e.g., North Anatolian fault [Stein *et al.*, 1997]), might rupture during great, clustered, earthquakes with long recurrence intervals. If characteristic events broke segments  $\approx 200$  km long, consistent with the large-scale linearity and continuity of the fault, each with 10 m of coseismic slip ( $M=8$ ), the corresponding recurrence time could be of order of 1000-2000 years. Since the very first earthquake in the historical catalog of Chinese earthquakes that is documented to be a  $M=8$  event is the Linfeng earthquake of 1303 A.D. [Gu *et al.*, 1989], a very large event on the RRF more than 1000 years ago would probably have been missed or not identified as such.

The tributaries of the Red River appear to have recorded cumulative motion on the RRF for at least several million years. There are several examples of large river courses that appear to have been stable for periods of millions of years and whose offsets across faults such as the Karakorum, the Haiyuan, or North Anatolian faults yield lower bounds of cumulative fault displacements [Gaudemer *et al.*, 1989; 1995] (see also Lacassin *et al.* [1998] for offsets of the Mekong and Salween by faults in the Golden Triangle). It is rarer, however, that relatively small drainage systems keep a record of large cumulative fault offsets. Here, the deep entrenchment of the rivers in the Ailao Shan range probably preserved the stability of the drainage network. Our work thus adds to the relatively small number of studies that address the problem of long-term drainage system evolution in tectonically active regions and steep mountain environments.

**Acknowledgments.** This work has been supported by Tectoscope program of CNRS-INSU and UMR7578 of CNRS. We have obtained detailed topographic data and field observations during cooperation between Academia Sinica and CNRS. We thank M. Klein from Total to permit us to work on seismic lines in Tonkin Gulf. We thank R. J. Norris and E. Fielding for detailed and constructive reviews. IPGP contribution N°1689.

## References

- Academy of Geological Sciences of China, Geological map of Asia, scale 1:5 000 000, Beijing, 1975.
- Allen, C. R., A. R. Gillespie, Y. Han, K. E. Sieh, B. Zhang, and C. Zhu, Red River and associated faults, Yunnan province, China: Quaternary geology, slip rates, and seismic hazard, *Geol. Soc. Am. Bull.*, **95**, 686-700, 1984.
- Allen, C. R., L. Zhuoli, Q. Hong, W. Xueze, Z. Huawei, and H. Weishi, Field study of a highly active fault zone: The Xianshuihe fault of southwestern China, *Geol. Soc. Am. Bull.*, **103**, 1178-1199, 1991.
- Armijo, R., P. Tapponnier, J. L. Mercier, and H. Tonglin, Quaternary extension in southern Tibet: Field observations and tectonic implications, *J. Geophys. Res.*, **91**, 13,803-13,872, 1986.
- Armijo, R., P. Tapponnier, and H. Tonglin, Late Cenozoic right-lateral strike-slip faulting in southern Tibet, *J. Geophys. Res.*, **94**, 2787-2838, 1989.
- Avouac, J.-P., and P. Tapponnier, Kinematic model of active deformation in central Asia, *Geophys. Res. Lett.*, **20**, 895-898, 1993.
- Briais, A., P. Patriat, and P. Tapponnier, Updated interpretation of magnetic anomalies and seafloor spreading stages in the South China Sea: Implications for the Tertiary tectonics of SE Asia, *J. Geophys. Res.*, **98**, 6299-6328, 1993.

- Chen, W. and Li Q., New evidences of tectonic uplift and transform of movement style along Ailao Shan-Red River fault Zone, *Chi. Sci. Bull.*, 43, 24, 1998.
- Duong, C. C. and K. Feigl, Geodetic measurement of horizontal strain across the Red River fault near Thac Ba, Vietnam, 1963-1994, *J. Geod.*, 73, 298-310, 1998.
- England, P., and P. Molnar, Right-lateral shear and rotation as the explanation for strike-slip faulting in eastern Tibet, *Nature*, 344, 140-142, 1990.
- Gaudemer, Y., P. Tapponnier, and D. L. Turcotte, River offsets across active strike-slip faults, *Ann. Tectonics*, 3, 55-76, 1989.
- Gaudemer, Y., P. Tapponnier, B. Meyer, G. Peltzer, Guo S., Chen Z., Dai H., and I. Cifuentes, Partitioning of crustal slip between linked, active faults in the eastern Qilian Shan, and evidence for a major seismic gap, the "Tianzhu gap", on the western Haiyuan Fault, Gansu (China), *Geophys. J. Int.*, 120, 599-645, 1995.
- Gu G., Lin T., Shi Z., Li Q., Wu H., Lu S., Yang Y., Chen H., and Wang S. (Eds.), *Catalogue of Chinese Earthquakes (1931 B.C.-1969 A.D.)*, pp. 872, Science Press, Beijing, China, 1989.
- Guo S., Zhang J., and Li X., Fault displacement and recurrence intervals of earthquakes on the northern segment of the honghe river fault zone, Yunnan province, *Seis. Geol.*, 8, 77-90, 1986.
- Harrison, T. M., P. H. Leloup, F. J. Ryerson, P. Tapponnier, R. Lacassin, and Chen W., Diachronous initiation of Transtension along the Ailao Shan-Red River Shear zone, Yunnan and Vietnam, in *The Tectonics of Asia*, edited by A. Yin and T. M. Harrison, pp. 208-226, Cambridge Univ. Press, New York, 1996.
- Heki, K., Horizontal and vertical crustal movements from three-dimensional very long baseline interferometry kinematic reference frame: Implication for the reversal timescale revision, *J. Geophys. Res.*, 101, 3187-3198, 1996.
- King, R. W., F. Shen, B. C. Burchfield, L. H. Royden, E. Wang, Z. Chen, Y. Liu, X.-Y. Zhang, J.-X. Zhao, and Y. Li, Geodetic measurement of crustal motion in southwest China, *Geology*, 25, 179-182, 1997.
- Lacassin, R., P. Tapponnier, P. H. Leloup, P. T. Trinh, and N. T. Yem, Morphotectonic evidence for active movements along the Red-River fault zone, in *International Workshop on Seismotectonics and Seismic Hazard in SE Asia*, pp. 66-71, Hanoi, Vietnam, 1994.
- Lacassin, R., A. Replumaz, and P. H. Leloup, Hairpin river loop and slip sense inversion on SE-Asian strike-slip faults, *Geology*, 26, 703-706, 1998.
- Leloup, P. H., Cinématique des déformations himalayennes dans la zone de cisaillement crustal de l'Ailao Shan-Fleuve Rouge, Thesis, Univ. Paris VI, 1991.
- Leloup, P. H., T. M. Harrison, F. J. Ryerson, W. Chen, L. Qi, P. Tapponnier, and R. Lacassin, Structural, petrological and thermal evolution of a Tertiary ductile strike-slip shear zone, Diancang Shan, Yunnan, *J. Geophys. Res.*, 98, 6715-6743, 1993.
- Leloup, P. H., P. H. Tapponnier, R. Lacassin, T. M. Harrison, and F. Ryerson, Diachronic uplift, transtension, and sinistral shear rate along the Red River zone, *Eos Trans. AGU*, 75 (44), Fall Meet. Suppl., 630, 1994.
- Leloup, P. H., R. Lacassin, P. Tapponnier, Zhong Dalai, Liu Xiaohan, Zhang Lianshang, Ji Shaocheng, and Phan Trong Trinh, The Ailao Shan-Red River shear zone (Yunnan, China), Tertiary transform boundary of Indochina, *Tectonophysics*, 251, 3-84, 1995.
- Liu, Q., J. P. Avouac, P. Tapponnier, and Q. Zhang, Holocene movement along the southern part of the Karakorum fault, in *International Symposium on the Karakorum and Kunlun Mountains*, p. 40, Kashgar, China, 1992.
- Liu, Q., Paléoclimat et contraintes chronologiques sur les mouvements récents dans l'Ouest du Tibet: failles du Karakorum et de Longmu Co-Gozha Co, lacs en pull-apart de Longmu Co et de Sumxi Co, Thesis, Univ. Paris VII, 1993.
- Molnar, P., and J. M. Gipson, A bound on the rheology of continental lithosphere using very long baseline interferometry: The velocity of south China with respect to Eurasia, *J. Geophys. Res.*, 101, 545-553, 1996.
- Peltzer, G., and F. Saucier, Present-day kinematics of Asia derived from geologic fault rates, *J. Geophys. Res.*, 101, 27,943-27,956, 1996.
- Peltzer, G., and P. Tapponnier, Formation and evolution of strike-slip faults, rifts, and basins during India-Asia collision: An experimental approach, *J. Geophys. Res.*, 93, 15,085-15,117, 1988.
- Peltzer, G., P. Tapponnier, Zhang Z., and Xu Z. Q., Neogene and quaternary faulting in and along the Qinling shan, *Nature*, 317, 500-505, 1985.
- Peltzer, G., P. Tapponnier, Y. Gaudemer, B. Meyer, S. Guo, K. Yin, Z. Chen, and H. Dai, Offsets of late Quaternary morphology, rate of slip, and recurrence of large earthquakes on the Changma fault (Gansu, China), *J. Geophys. Res.*, 93, 7793-7812, 1988.
- Peltzer, G., P. Tapponnier, and R. Armijo, Magnitude of late Quaternary left-lateral displacements along the northern edge of Tibet, *Science*, 246, 1285-1289, 1989.
- Replumaz, A., Tectonique active du Vietnam, DEA report, Univ. Paris VII, 1994.
- Scharer, U., P. Tapponnier, R. Lacassin, P. H. Leloup, Zhong D., and Ji S., Intraplate tectonics in Asia: a precise age for large-scale Miocene movement along the Ailao Shan-Red River shear zone, China, *Earth Planet. Sci. Lett.*, 97, 65-77, 1990.
- Scharer, U., L.-S. Zhang, and P. Tapponnier, Duration of strike-slip movements in large shear zones: The Red River belt, China, *Earth Planet. Sci. Lett.*, 126, 379-397, 1994.
- Stein, R., A. A. Barka, and J. H. Dieterich, Progressive failure on the North Anatolian fault since 1939 by earthquakes stress triggering, *Geophys. J. Int.*, 128, 594-604, 1997.
- Tapponnier, P., and P. Molnar, Active faulting and tectonics in China, *J. Geophys. Res.*, 82, 2905-2930, 1977.
- Tapponnier, P., G. Peltzer, R. Armijo, A.-Y. Le Dain, and P. Cobbold, Propagating extrusion tectonics in Asia: new insights from simple experiments with plasticine, *Geology*, 10, 611-616, 1982.
- Tapponnier, P., G. Peltzer, and R. Armijo, On the mechanics of the collision between India and Asia, in *Collision Tectonics*, edited by J. G. Ramsay, M. P. Coward, and A. C. Ries, *Geol. Soc. Spe. Publ.*, 19, 115-157, 1986.
- Tapponnier, P., R. Lacassin, P. H. Leloup, U. Schärer, Zhong D., Liu X., Ji S., Zhang L., and Zhong J., The Ailao Shan/Red River metamorphic belt: Tertiary left-lateral shear between Indochina and south China, *Nature*, 343, 431-437, 1990.
- Weldon, R., K. Sieh, Zhu C., Han Y., Yang J., and S. Robinson, Slip rate and recurrence interval of earthquake on the Hong He (Red River) Fault, Yunnan, P.R.C., in *International Workshop on Seismotectonics and Seismic Hazard in SE Asia*, pp. 244-248, Hanoi, Vietnam, 1994.
- Zhang, Y., P. Vergely, and J. Mercier, Active faulting in and along the Qinling range (China) inferred from SPOT imagery analysis and extrusion tectonics of south China, *Tectonophysics*, 243, 69-95, 1995.

A. Replumaz, Laboratoire de Géophysique Interne et Tectonophysique, Observatoire de Grenoble, CNRS UMR 5559, BP 53X, 38000 Grenoble, France. (Anne.Replumaz@obs.ujf-grenoble.fr)

R. Lacassin, P. H. Leloup, and P. Tapponnier, Institut de Physique du Globe de Paris, CNRS UMR 7578, 4 place Jussieu, 75252 Paris cedex 05, France. (lacassin@ipgp.jussieu.fr; lelou@ipgp.jussieu.fr; tappon@ipgp.jussieu.fr)

(Received May 12, 1999; revised January 20, 2000; accepted April 10, 2000)